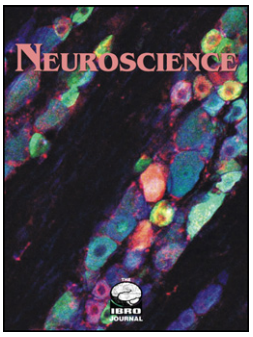

Amyotrophic lateral sclerosis mutant VAPB transgenic mice develop TDP-43 pathology

Elizabeth L. Tudor, Clare M. Galtrey, Michael S. Perkinton, Kwok-Fai Lau, Kurt J. De Vos, Jacqueline C. Mitchell, Steven Ackerley, Tibor Hortobágyi, Eniko Vámos, P. Nigel Leigh, Christian Klasen, Declan M. McLoughlin, Christopher E. Shaw, Christopher C.J. Miller

PII: S0306-4522(10)00263-0
DOI: 10.1016/j.neuroscience.2010.02.035
Reference: NSC 11895

To appear in: *Neuroscience*

Received date: 2 November 2009
Revised date: 9 February 2010
Accepted date: 12 February 2010

Please cite this article as: Tudor, E.L., Galtrey, C.M., Perkinton, M.S., Lau, K.F., De Vos, K.J., Mitchell, J.C., Ackerley, S., Hortobágyi, T., Vámos, E., Leigh, P.N., Klasen, C., McLoughlin, D.M., Shaw, C.E., Miller, C.C.J., Amyotrophic lateral sclerosis mutant VAPB transgenic mice develop TDP-43 pathology, *Neuroscience* (2009), doi: 10.1016/j.neuroscience.2010.02.035.

Amyotrophic lateral sclerosis mutant VAPB transgenic mice develop TDP-43 pathology

Elizabeth L. Tudor[1]*, Clare M. Galtrey[1]*, Michael S. Perkinton[1], Kwok-Fai Lau[1,2], Kurt J. De Vos[1], Jacqueline C. Mitchell[1], Steven Ackerley[1], Tibor Hortobágyi[1], Enikő Vámos[1], P. Nigel Leigh[1], Christian Klasen[3], Declan M. McLoughlin[1,4], Christopher E. Shaw[1] and Christopher C.J. Miller[1]

* These authors contributed equally to this work

[1] MRC Centre for Neurodegeneration Research, Institute of Psychiatry, King's College, London, Denmark Hill, London SE5 8AF, UK.

[2] Department of Biochemistry, The Chinese University of Hong Kong, Shatin, NT, Hong Kong.

[3] Biology Unit, European Molecular Biology Laboratory, Meyerhofstrasse 1, 69117, Heidelberg Germany.

[4] Department of Psychiatry and Trinity College Institute of Neuroscience, Trinity College Dublin, St Patrick's Hospital, James's Street, Dublin 8, Ireland

Correspondence to: Chris Miller, MRC Centre for Neurodegeneration Research, Department of Neuroscience P037, Institute of Psychiatry, De Crespigny Park, Denmark Hill, London SE5 8AF, UK.

Email: chris.miller@kcl.ac.uk; Tel. +44(0)207 8480393; Fax +44(0)207 7080017

Section Editor: (Molecular Neuroscience) L. Kaczmarek, Dept. of Molecular and Cellular Neurobiology, Nencki Institute of Experimental Biology, ul. Pasteura 3, 02-093 Warsaw, Poland

Abbreviations used: VAPB, vesicle-associated membrane protein-associated protein-B; TDP-43, TAR-DNA-binding protein-43; ALS, amyotrophic lateral sclerosis; SOD1, copper/zinc superoxide dismutase-1; UPR, unfolded protein response; FTLD, fronto-temporal lobar degeneration; MSP1, major sperm protein-1.

Abstract

Cytoplasmic ubiquitin-positive inclusions containing TAR-DNA-binding protein-43 (TDP-43) within motor neurons are the hallmark pathology of sporadic amyotrophic lateral sclerosis (ALS). TDP-43 is a nuclear protein and the mechanisms by which it becomes mislocalised and aggregated in ALS are not properly understood. A mutation in the vesicle-associated membrane protein-associated protein-B (VAPB) involving a proline to serine substitution at position 56 (VAPBP56S) is the cause of familial amyotrophic lateral sclerosis (ALS) type-8. To gain insight into the molecular mechanisms by which VAPBP56S induces disease, we created transgenic mice that express either wild-type VAPB (VAPBwt) or VAPBP56S in the nervous system. Analyses of both sets of mice revealed no overt motor phenotype nor alterations in survival. However, VAPBP56S but not VAPBwt transgenic mice develop cytoplasmic TDP-43 accumulations within spinal cord motor neurons that were first detected at 18 months of age. Our results suggest a link between abnormal VAPBP56S function and TDP-43 mislocalisation.

Keywords: Motor neuron disease; vesicle-associated membrane protein-associated protein-B; TAR-DNA-binding protein-43; ubiquitin.

Introduction

ALS is a fatal neurodegenerative disease that involves selective loss of motor neurons. Most forms of ALS are sporadic but about 10% are familial and a number of genetic lesions have now been identified that are causative for these inherited forms of the disease (Pasinelli and Brown, 2006, Valdmanis and Rouleau, 2008, Kwiatkowski et al., 2009, Vance et al., 2009). Mutations in the gene encoding Cu/Zn superoxide dismutase-1 (SOD1) account for approximately 20% of the familial cases and expression of mutant but not wild-type SOD1 in transgenic mice can induce motor neuron disease (Boillee et al., 2006). Analyses of such mice have provided crucial insights into the pathogenic mechanisms that underlie ALS.

One hallmark pathology of ALS is cytoplasmic ubiquitin inclusions containing TDP-43 within motor neurons (Arai et al., 2006, Neumann et al., 2006). TDP-43 is a ubiquitously expressed nuclear protein that is implicated in exon splicing, gene transcription, mRNA stability, microRNA biogenesis and the formation of nuclear bodies (Ou et al., 1995, Wang et al., 2002, Ayala et al., 2006, Ayala et al., 2008, Buratti and Baralle, 2008). Moreover, several groups have reported mutations in TDP-43 that are linked to familial and sporadic forms of ALS (Gitcho et al., 2008, Kabashi et al., 2008, Sreedharan et al., 2008, Van Deerlin et al., 2008, Yokoseki et al., 2008). This evidence formally links aberrant TDP-43 function to ALS. The mechanisms by which TDP-43 becomes mislocalised within the cytoplasm of motor neurons in ALS are not properly understood. Interestingly, TDP-43 pathology is not prominent in either the human mutant SOD1 familial cases or transgenic mice expressing mutant SOD1 (Mackenzie et al., 2007, Robertson et al., 2007, Tan et al., 2007, Turner et al., 2008). Recent studies however have provided evidence that TDP-43 can mislocalise in some human mutant SOD1 familial cases and mutant SOD1 transgenic mice (Shan et al., 2009, Sumi et al., 2009).

A mutation in VAPB is the cause of a further familial form of ALS (ALS8) (Nishimura et al., 2004). VAP proteins were first identified in Aplysia as a binding partner for VAMP, a membrane protein in synaptic vesicles (Skehel et al., 1995). Structurally, VAPB contains an N-terminal domain that is homologous to the filament-forming major sperm protein-1 (MSP1) of nematode worms, a central coiled-coil region and a C-terminal transmembrane domain. The disease causing mutation involves a proline to serine substitution at position 56 (VAPBP56S); proline-56 is highly conserved and resides within the MSP1 domain.

VAPB localises to the endoplasmic reticulum (ER) but there is evidence that a proportion is also associated with microtubules (Skehel et al., 2000, Pennetta et al., 2002, Amarilio et al., 2005, Kanekura et al., 2006, Teuling et al., 2007). However, the precise function of VAPB is not properly understood. It is implicated in bouton formation at the neuromuscular junction, ER to Golgi transport and ER stress and the unfolded protein response (UPR) (Pennetta et al., 2002, Kanekura et al., 2006, Gkogkas et al., 2008, Peretti et al., 2008, Prosser et al., 2008, Ratnaparkhi et al., 2008, Suzuki et al., 2009). Finally, VAPB has also been shown to be cleaved and secreted and act as a ligand for ephrin receptors (Tsuda et al., 2008). Whether defects in any of these functions induces motor neuron disease is not clear but VAPBP56S displays an altered cellular distribution and forms ER-derived aggregates that also contain wild-type VAPB (Kanekura et al., 2006, Teuling et al., 2007, Chai et al., 2008, Gkogkas et al., 2008). This has prompted the suggestion that VAPBP56S acts as a loss-of-function mutant (Teuling et al., 2007, Ratnaparkhi et al., 2008, Suzuki et al., 2009).

One route to understand further how VAPBP56S might cause disease would be to determine whether it is linked to other known pathogenic processes involved in ALS. To this end, we created transgenic mice expressing wild-type VAPB (VAPBwt) or VAPBP56S to permit analyses of in vivo phenotypic changes. We find that VAPBP56S but not VAPBwt

transgenic mice develop cytoplasmic TDP-43 and ubiquitin pathologies in motor neurons. Our results suggest that VAPBP56S is linked to defective TDP-43 metabolism.

Experimental Procedures

Molecular biology and creation of transgenic mice

A human VAPBP56S cDNA was created using a Quickchange mutagenesis kit (Stratagene) and N-terminal myc tags of both VAPBwt and VAPBP56S generated by PCR. For creation of transgenic mice, myc-tagged VAPBwt and VAPBP56S cDNAs were cloned into a modified mouse prion gene and following removal of vector sequences, mice were produced by pronuclear injection as described (Lee et al., 2003). Animals were backcrossed to C57Bl/6 for four times prior to analyses. Mice were identified using PCR with primers 5'-ATGGAGCAGAAACTCATCTCTGAAGAGGATCTGATGGCGAAG-3' and 5'-GTCAAGGCCTTCTTCCTTCCCAGTTGGGGC-3'. SOD1G93A transgenic mice were obtained from the Jackson Laboratory (Bar Harbor, ME) and were back-crossed to C57BL/6 for 10 generations. Genotyping of SOD1G93A mice was performed as described (De Vos et al., 2007).

Antibodies and other reagents

Rat and rabbit antibodies to VAPB were created by immunisation of animals with residues 1-219 of human VAPB expressed as a GST-fusion protein. Mouse and human VAPB display approximately 95% homology over this region and as such, these VAPB antibodies are not species-specific. Antibodies were affinity purified against antigen and immunoblots demonstrated that both antibodies detected a single species in brain and spinal cord tissues that co-migrated with VAPB in transfected cells (data not shown). The following commercially-available antibodies were used: myc-tag antibodies 9B11 (Cell Signaling Technology) and 9E10 (Sigma); neurofilament antibody SMI31 (Biomol International); ubiquitin mouse monoclonal (Ubi-1, Millipore) and rabbit polyclonal (DAKO) antibodies;

p62 Lck Ligand mouse monoclonal antibody (BD Transduction Laboratories); TDP-43 rabbit polyclonal antibody (Proteintech); DM1A mouse monoclonal tubulin antibody (Sigma).

Immunohistochemical analyses

Mice were terminally anesthetized with an intraperitoneal overdose of Euthatal (sodium pentobarbital) and were immediately perfused through the heart with 50 ml cold 0.1 M phosphate-buffer (pH 7.4), followed by 50 ml cold 4% paraformaldehyde in phosphate buffered saline and the brain and spinal cord removed. Tissues were postfixed for 3-4 hours in 4% paraformaldehyde then processed for paraffin embedding. 7 μm sections were cut on a Leica microtome, mounted onto Superfrost Plus slides (VWR International) and dried at 37^{O}C for 16 hours. The slides were then stored at room temperature until required.

Sections were deparaffinized in xylene and hydrated in graded alcohol. For immunoperoxidase labelling, endogenous peroxidase activity was blocked with H_2O_2 in methanol. Antigen retrieval was performed on all sections by microwave incubation in citrate buffer. Sections were then incubated in 15% normal goat serum (Vector Laboratories) for 30 minutes in Tris-buffered saline (TBS; 50 mM Tris(hydroxymethyl)aminomethane-HCl containing 150 mM NaCl pH 7.6) at 22^{o}C, and then primary antibodies for 16 hours at 4^{o}C in TBS containing 10% normal goat serum. For experiments involving mouse primary antibodies, signals from endogenous mouse immunoglobulins were blocked by incubation with unconjugated Affinipure Fab fragment of goat anti-mouse IgG (H=L) (Jackson ImmunoResearch Labs). For immunoperoxidase labelling, sections were incubated with biotinylated secondary antibodies (Vector laboratories; DAKO) followed by signal amplification using avidin-biotin horseradish peroxidase complex (Vectastain ABC Elite kit, Vector Laboratories) and the reaction product was visualized with the chromogen

diaminobenzidine (DAB; Sigma). Sections were counterstained with haematoxylin, washed in water and then dehydrated, cleared in xylene and mounted in DPX mountant for microscopy (VWR International).

For immunofluorescence studies, following incubation with primary antibodies, sections were incubated with species-specific secondary antibodies generated in goat and conjugated to Alexa Fluor® 488, 546 or 633 (Invitrogen). For mouse primary antibodies, sections were incubated with a Biotin-SP-conjugated AffiniPure Fab fragment goat anti-mouse IgG (H+L) (Jackson ImmunoResearch Labs) followed by a streptavidin-Alexa Fluor® 488 or 546 conjugate (Invitrogen). Some sections were co-stained with 4',6' diamidino-2-phenylindole to label nuclei (Invitrogen). Sections were mounted in fluorescence mounting medium (DAKO).

Images were captured on a Zeiss Axiovert microscope equipped with an Axiocam MRc camera. For immunofluorescence studies, confocal images were acquired using a Zeiss LSM 510 meta confocal microscope with a photomultipler detector.

Motor neuron counts were determined as described by others (Feeney et al., 2001, Zhou et al., 2007, Ilieva et al., 2008). Briefly, 20 μm sections were prepared through the spinal cord and every tenth section stained with 1% cresyl violet and used for motor neuron counts. Images were captured and motor neurons identified and quantified manually using Image J as described by others (motor neurons were identified by having a prominent nucleolus, a clearly defined cytoplasm and a cell somal area greater than 100 μm^2) (McHanwell and Biscoe, 1981, Feeney et al., 2001, Zhou et al., 2007, Ilieva et al., 2008). Statistical significance was determined using one-way ANOVA and Holm-Sidak post hoc analysis.

Image analyses

Quantitative image correlation analyses were performed essentially as described (Li et al., 2004). For comparisons of signal distributions from different markers (ubiquitin, TDP-43 and VAPB), intensity correlation quotients (ICQs) were generated and used for statistical analyses. ICQ analyses were carried out by means of a custom-made plug-in for the public domain image analysis software Image J (Wayne Rasband, Research Services Branch, National Institute of Mental Health, NIH Bethesda MD). Statistical significance was determined using one-sample t-test.

SDS-PAGE and immunoblotting

Brain and spinal cord tissues were weighed and prepared as 10% (w/v) homogenates in ice-cold 20 mM Tris-Cl (pH 6.8), 5 mM EDTA, 5 mM EGTA supplemented with complete protease inhibitor mixture (Roche Applied Science), 1 mM PMSF and 1 mM sodium orthovanadate. 10% SDS sample buffer was then added, and the samples were heated at 95^{O}C for 10 min. Samples were resolved by SDS-PAGE on 10% or 12% gels, transferred to nitrocellulose using a BioRad Transblot system and the blots probed with primary and secondary antibodies and developed using an enhanced chemiluminescence system (GE Healthcare) as described (Tudor et al., 2005). For TDP-43 cleavage studies, samples were prepared as described (Neumann et al., 2006). Protein concentrations were determined using Bradford assay.

Neurological testing of mice

Neurological testing was performed on cohorts of animals aged 6-8, 12-14 and 22-24 months of age (n= 12-15 for all tests). Mice were analysed for neurological defects using the primary SHIRPA screen (Rogers et al., 1997). These included assessment of motor

phenotype using grip-strength and rotating rod (Rotarod) tests that were performed in similar fashions to those reported by many other groups (e.g. (Fowler et al., 2002, Puttaparthi et al., 2002, Fischer et al., 2005, Nakajima et al., 2008)). Briefly, fore and hind limb grip-strengths were assessed using a Linton Grip Strength Meter (Linton Instrumentation, UK). Mice received three trials per day for three days, and the best results of each day were averaged to give the final result. Rotarod tests were performed using an Ugo Basile accelerating Rotarod (Linton Instrumentation, UK). Mice were tested for 300 s in the accelerating paradigm (5-40 rpm) twice per day for 7 days and the best performance of each day was averaged to give the final result. Performance on the balance beam was determined as described (Lalonde and Strazielle, 2009).

Human Tissues

Human tissues were obtained from the MRC London Neurodegenerative Disease Brain Bank. Informed consent was obtained from the families of patients in accordance with the stipulations and guidance of the Committee for Ethics in Medical Research, Institute of Psychiatry, King's College London, and in line with the Human Tissue Authority's and Medical Research Council's brain-banking procedures for the removal of the brain and spinal cord and use of tissue in research.

Results

Characterisation of transgenic mice expressing VAPBwt and VAPBP56S

We created VAPBwt and VAPBP56S transgenic mice using the mouse prion gene promoter and regulatory elements as previously described; the prion gene is known to drive expression within the nervous system (Lee et al., 2003, Lee et al., 2004). To facilitate detection, we placed a myc tag on the N-terminus of both VAPB constructs. We obtained 4 VAPBwt and 5 VAPBP56S transgenic lines. Probing of immunoblots with antibody 9B11 to the myc tag and with the different rabbit and rat antibodies to VAPB revealed that all lines expressed approximately similar levels of transgenic VAPB protein in brains and spinal cords. We therefore selected two VAPBwt and two VAPBP56S lines for further study. Quantification of signals from the VAPB antibodies in brain and spinal cord samples revealed that VAPB was overexpressed to similar levels in each of the VAPBwt and VAPBP56S transgenic lines (Fig. 1).

To analyse VAPBwt and VAPBP56S expression in more detail, we immunostained sections of brains and spinal cords with an antibody to the myc tag. These studies revealed indistinguishable patterns of labelling for both VAPBwt lines with transgenic VAPBwt being present in a number of different neuronal populations within the brain and spinal cord including motor neurons in spinal cords (Fig. 2). Likewise, expression of VAPBP56S was not noticeably different in the two lines studied; expression was observed in different neuronal populations in the brain and spinal cord with labelling of motor neurons in spinal cords again being prominent (Fig. 2). Higher magnification images revealed that whilst VAPBwt was distributed throughout the neuronal cytoplasm, VAPBP56S was additionally present within punctate accumulations in a similar fashion to that previously observed following transfection into cultured cells (Nishimura et al., 2004, Kanekura et al., 2006,

Teuling et al., 2007, Gkogkas et al., 2008) (Fig. 2). These VAPBP56S accumulations were seen in both brain and spinal cord neurons including motor neurons (Fig. 2C, E).

Neither VAPBwt nor VAPBP56S transgenic mice develop overt motor neuron disease

We monitored weight and lifespan (up to 2 years) of VAPBwt, VAPBP56S and their non-transgenic littermates but detected no significant differences between the different transgenic and non-transgenic animals. To determine whether VAPBwt or VAPBP56S transgenic mice develop neurological dysfunction and especially motor function, we utilised aspects of the SHIRPA primary protocol (Rogers et al., 1997) including rotarod and fore and hind leg grip-strength tests. These tests were performed on cohorts of animals aged 6-8, 12-14 and 22-24 months of age (n= 12-15 for all tests). No significant differences were obtained between the various genotypes at either age. We also quantified motor neuron numbers in spinal cords of VAPBwt, VAPBP56S and their non-transgenic littermates at 24 months of age (n=3). However, we again detected no significant differences between the genotypes. Thus, moderate overexpression of either VAPBwt or VAPBP56S in brain and spinal cord does not induce major motor dysfunction or overt motor neuron disease in mice.

VAPBP56S but not VAPBwt transgenic mice develop cytoplasmic ubiquitin and TDP-43 pathologies

Accumulations of neurofilaments and ubiquitin-positive cytoplasmic TDP-43 inclusions are prominent features of ALS (Al-Chalabi and Miller, 2003, Neumann et al., 2006). Despite the absence of overt motor neuron disease, we therefore investigated whether any pathological changes in neurofilament, ubiquitin or TDP-43 labelling occurred in spinal cords of VAPB transgenic mice. We analysed mice at 6 month, 12 months, 18 months and 24

months. No noticeable differences in patterns of neurofilament staining were detected between VAPBwt, VAPBP56S and non-transgenic littermates at ages of up to 24 months (data not shown). However, at 18 months of age but not before, both VAPBP56S transgenic lines but not the VAPBwt transgenic lines displayed increased cytoplasmic labelling for ubiquitin within spinal cord motor neurons (Fig. 3). Higher magnification images revealed that this ubiquitin labelling was granular in appearance and associated with discrete areas of cytoplasm (Fig. 3B). For comparison, we also stained SOD1G93A transgenic mice for ubiquitin and TDP-43 and detected strongly labelled ubiquitin-positive inclusions within motor neurons but no overt TDP-43 pathology which is similar to previous studies (Robertson et al., 2007, Turner et al., 2008) (Fig. 3A and Fig. 4A). We also labelled sections for p62 which is a ubiquitin binding protein that is associated with ubiquitin inclusions, including ubiquitin/TDP-43 inclusions in ALS (Mizuno et al., 2006, Seelaar et al., 2007). Again, granular-like p62 labelling of discrete areas of cytoplasm was observed in motor neurons of VAPBP56S but not VAPBwt or non-transgenic mice (Fig. 3C).

Immunostaining for TDP-43 produced prominent nuclear labelling in non-transgenic, VAPBwt and VAPBP56S transgenic mice consistent with its known distribution. However, in spinal cord motor neurons of VAPBP56S but not VAPBwt or non-transgenic littermates we additionally detected the presence of cytoplasmic TDP-43 positive labelling (Fig. 4A). This abnormal TDP-43 labelling became noticeable in 18 month old mice, the same age as the ubiquitin pathology first appeared and was localised to discrete regions of cytoplasm again similar to that seen for ubiquitin and p62 (Fig. 4A). In some neurons, we also observed a diffuse general increase in cytoplasmic TDP-43 (Fig. 4B). Analyses of 24 month old VAPBP56S mice revealed similar changes. Indeed, we detected no noticeable

differences in ubiquitin, p62 and TDP-43 cytoplasmic labelling between 18 month old and 2 year old VAPBP56S mice.

For comparative purposes, we additionally investigated TDP-43 pathology in human ALS spinal cord. This involved analyses of a 43-year old female who died with clinical features of motor neuron disease and frontotemporal dementia. Histological analyses confirmed motor neuron disease with frontotemporal lobar degeneration with TDP-43 positive inclusions. Concordant with previous studies, we found robust cytoplasmic TDP-43 pathological inclusions within motor neurons. Noteably however, these inclusions were more intensely stained and of a more defined structure than those seen in VAPBP56S transgenic mice. Rather, TDP-43 cytoplasmic abnormalities in VAPBP56S transgenic mice appeared more granular and diffusely labelled; skein like inclusions and large round aggregates as seen in human cases were not detected. This was the case for both 18 month and 24 month old VAPBP56S mice.

Co-localisation of cytoplasmic ubiquitin with TDP-43 in VAPBP56S transgenic mice

To determine whether the cytoplasmic TDP-43 and ubiquitin pathologies seen in VAPBP56S mice motor neurons were in any way related, we triple immunostained sections for TDP-43, ubiquitin and VAPB, and analysed the labelling by confocal microscopy. In VAPBwt transgenic animals, TDP-43 labelling was again restricted to the nucleus and VAPB labelling localised to the cytoplasm (Fig. 5A). These results were thus identical to those observed by conventional marker labelling and as described above (Figs. 2, 3, 4). However, in VAPBP56S transgenic mice, TDP-43 labelling was also detected in the cytoplasm and in overlay images, this labelling appeared similar to that for ubiquitin (Fig. 5B).

Although conventional dye-overlay methods generate visual estimates of co-distribution, these methods can report incorrect co-localisation of two proteins. This is because they do not take into account the relative proportions of signals from different proteins which in the case of co-localisation, should vary in synchrony. We therefore determined the co-localisation of TDP-43 and ubiquitin, and VAPB and ubiquitin by image correlation analyses (Li et al., 2004). Image correlation analysis compares the scatter plots of two stains against the product of the difference of the pixel intensities of each of the two stains from their respective means. Thus, image correlation analysis determines whether the pixel intensities from two signals vary in synchrony. In addition, the values obtained from the analysis can be reported as an image correlation quotient (ICQ), which is a statistically testable, single value assessment of the relationship between two stained protein pairs; for random staining ICQ=~0, for dependent staining (co-localisation) $0<ICQ\leq+0.5$, and for segregated staining $0>ICQ\geq-0.5$.

The image correlation analysis showed that in aged (18 month and 24 month old) VAPBP56S mice, TDP-43 co-localised highly significantly with ubiquitin within the cytoplasmic aggregates (Fig. 5C; ICQ=0.22±0.06; ICQ>0, $p<0.001$, "One sample t test", n=17 cells). It has been reported that VAPB can also be ubiquitinated (Tsuda et al., 2008). We therefore analyzed co-localisation of VAPB and ubiquitin in the same neurons. VAPB and ubiquitin were also significantly co-localised (ICQ=0.16±0.05; ICQ>0, $p<0.001$, "One sample t test", n=17). However, co-localisation of ubiquitin with TDP-43 was significantly greater than ubiquitin and VAPB ($p=0.0188$, t-test, df=32; Fig. 5D). Thus, VAPBP56S transgenics develop TDP-43 and associated ubiquitin pathology similar to that seen in sporadic forms of ALS.

Absence of cleavage of TDP-43 in VAPBP56S transgenic mice

Cleavage of TDP-43 to generate carboxy-terminal fragments including 25 kDa species have been observed in ALS and frontotemporal lobar degeneration with ubiquitin inclusions (FTLD-U) (Neumann et al., 2006). However, this cleavage is restricted to brain and not spinal cord tissues (Igaz et al., 2008). We therefore enquired whether cleavage of TDP-43 occurred in spinal cords and/or brain of either VAPB or VAPBP56S transgenic mice. Probing of spinal cord samples from 24 month old VAPB, VAPBP56S and non-transgenic littermate mice revealed no differences in the migration TDP-43; no faster migrating species specific to either VAPB or VAPBP56S mice were detected (Fig. 6). Thus, despite the presence of TDP-43 pathology in spinal cords of VAPBP56S transgenic mice, we did not detect any proteolytic cleavage of TDP-43 and this is consistent with that seen in sporadic human ALS cases.

Discussion

Here, we describe the phenotype of ALS-causing VAPBP56S overexpressing transgenic mice. We compared two VAPBP56S and two VAPBwt transgenic lines. Both VAPBP56S and VAPBwt lines expressed broadly similar levels of transgenic protein. Neurological testing of the mice did not reveal any clear disease phenotype in either VAPB or VAPBP56S transgenics even in mice aged 24 months; neither did we detect any loss of motor neurons. Thus, expression of either VAPBP56S or VAPBwt to moderate levels does not induce overt motor neuron disease in mice. This is in contrast to mutant SOD1 where expression levels of mutant protein equal to, or less than the endogenous mouse protein (20% of endogenous) can induce aggressive motor neuron disease (Bruijn et al., 1997). The initial description of ALS8 involved seven kindreds with the VAPBP56S mutation. Of these, three developed late-onset slowly progressive atypical ALS, three developed late-onset spinal muscular atrophy, and in the final family only selected members developed typical ALS with others showing atypical ALS (Nishimura et al., 2004). Thus, absence of disease in VAPBP56S transgenic mice may reflect the less severe and late-onset disease phenotype observed in most ALS8 cases. Whether higher levels of VAPBP56S expression in mice can induce disease is not known. A further possibility is that disease may require expression of VAPBP56S in cell types within the nervous system in which the prion promoter used here is not active. Indeed motor neuron cell loss and robust disease in mutant SOD1 cases is now believed to be non-cell-autonomous and to require expression in cell-types other than motor neurons and in particular in microglia (Boillee et al., 2006). Similar events may be required for VAPBP56S-induced disease.

We observed cytoplasmic TDP-43 pathology in spinal cord motor neurons of VAPBP56S but not VAPBwt transgenic mice. This involved discrete cytoplasmic accumulations but also some diffuse, general increase in cytoplasmic TDP-43 labelling that developed first in 18

month old mice; no obvious enhancement of this pathology was seen in 24 month old mice. The appearance of this TDP-43 pathology coincided with the appearance of cytoplasmic ubiquitin accumulations and we utilised image correlation analyses to demonstrate that the two pathologies strongly co-localised. We also observed some co-localisation between ubiquitin and VAPB although the image correlation analyses produced lower scores than for ubiquitin and TDP-43.

We compared the TDP-43 pathology in VAPBP56S mice to that seen in human disease cases. In the human cases, TDP-43 pathology involved skein-like, round and elongated inclusions and to a lesser extent, diffuse granular labelling in anterior horn motor neurons. By contrast, cytoplasmic TDP-43 accumulations present in VAPBP56S mice were less intensely labelled and less well defined in structure. The redistribution of TDP-43 to the cytoplasm and its ubiquitination are now known to be early events in ALS and precede the formation of insoluble inclusion bodies (Giordana et al., 2009). Thus, one possibility is that the structurally less defined, granular cytoplasmic TDP-43 accumulations seen in VAPBP56S mice represent a relatively early stage in the development of pathology and this is consistent with the absence of neurological disease in these mice. Indeed, others have reported granular cytoplasmic TDP-43 pathologies in human fronto-temporal dementia with or without motor neuron disease and have concluded that they represent an early pre-inclusion pathology (Cairns et al., 2007).

The mechanisms by which both mutant SOD1 and VAPBP56S induce motor neuron cell demise are not properly understood. However, VAPB is an integral ER protein and several recent studies have provided evidence that it functions in protection against ER stress and in particular in UPR signalling (Skehel et al., 2000, Loewen and Levine, 2005, Kanekura et al., 2006, Teuling et al., 2007, Gkogkas et al., 2008, Suzuki et al., 2009). The UPR is a signalling

pathway that is activated by accumulation of unfolded proteins within the ER and which triggers transcriptional responses so as to rectify the protein folding capacity of the cell (Bernales et al., 2006). VAPB has been linked to the cell's ability to promote the UPR with VAPBP56S being defective in this function although paradoxically in Drosophila, VAPBP58S (the equivalent of VAPBP56S) is reported to promote UPR (Kanekura et al., 2006, Gkogkas et al., 2008, Tsuda et al., 2008). VAPBP56S mislocalises to ER-derived tubular aggregates which also contain wild-type VAPB and one possibility is that this recruitment of VAPB to aggregates diminishes the cell's UPR ability; as such VAPBP56S may function as a loss of function and/or dominant negative molecule so that the protective function of the UPR in response to ER stress is diminished in mutant expressing cells (Kanekura et al., 2006, Teuling et al., 2007, Gkogkas et al., 2008, Suzuki et al., 2009). Further support for a loss of function of VAPB contributing to ALS pathogenesis comes from the finding that VAPB levels are reduced in spinal cords of ALS cases (Anagnostou et al., 2008).

TDP-43 is synthesised within the ER and then trafficked to the nucleus and one suggestion is that the appearance of cytoplasmic TDP-43 pathology in ALS is a consequence of defects in this trafficking (Winton et al., 2008a, Winton et al., 2008b). Recently, ER stress has been linked to defective cytoplasmic/nuclear trafficking of TDP-43 in familial fronto-temporal lobar degeneration (FTLD) with inclusion body myopathy and Paget disease of bone that is caused by mutations in the valosin-containing protein (VCP) gene (Gitcho et al., 2009). Thus, one possibility is that as may be the case in the mutant VCP forms of FLTD, VAPBP56S induces cytoplasmic accumulation of TDP-43 via damage to the UPR and induction of ER stress such that TDP-43 trafficking to the nucleus in impaired. Whatever the

precise mechanism, our results reported here provide support for a link between ALS associated VAPBP56S and cytoplasmic accumulation of TDP-43.

Acknowledgements

This work was supported by grants from the MRC, Wellcome Trust, MNDA, EU Framework 6 NeuroNE, BBSRC, Alzheimer's Research Trust and Alzheimer's Association. CMG was supported by a grant from GlaxoSmithKline, and TH by a grant from The NIHR Biomedical Research Centre for Mental Health at the South London and Maudsley NHS Foundation Trust and the Institute of Psychiatry, King's College London. Human tissues were provided by the MRC London Neurodegenerative Diseases Brain Bank. We thank Boris Rogelj, Stephen Shemilt, Carl Hobbs and Mavis Kibble for assistance.

References

Al-Chalabi A, Miller CCJ (2003) Neurofilaments and neurological disease. Bioessays 25:346-355.

Amarilio R, Ramachandran S, Sabanay H, Lev S (2005) Differential regulation of endoplasmic reticulum structure through VAP-Nir protein interaction. J Biol Chem 280:5934-5944.

Anagnostou G, Akbar MT, Paul P, Angelinetta C, Steiner TJ, de Belleroche J (2008) Vesicle associated membrane protein B (VAPB) is decreased in ALS spinal cord. Neurobiol Aging.

Arai T, Hasegawa M, Akiyama H, Ikeda K, Nonaka T, Mori H, Mann D, Tsuchiya K, Yoshida M, Hashizume Y, Oda T (2006) TDP-43 is a component of ubiquitin-positive tau-negative inclusions in frontotemporal lobar degeneration and amyotrophic lateral sclerosis. Biochem Biophys Res Commun 351:602-611.

Ayala YM, Misteli T, Baralle FE (2008) TDP-43 regulates retinoblastoma protein phosphorylation through the repression of cyclin-dependent kinase 6 expression. Proc Natl Acad Sci USA 105:3785-3789.

Ayala YM, Pagani F, Baralle FE (2006) TDP43 depletion rescues aberrant CFTR exon 9 skipping. FEBS Lett 580:1339-1344.

Bernales S, Papa FR, Walter P (2006) Intracellular signaling by the unfolded protein response. Annu Rev Cell Dev Biol 22:487-508.

Boillee S, Vande Velde C, Cleveland DW (2006) ALS: A disease of motor neurons and their nonneuronal neighbors. Neuron 52:39-59.

Bruijn LI, Becher MW, Lee MK, Anderson KL, Jenkins NA, Copeland NG, Sisodia SS, Rothstein JD, Borchelt DR, Price DL, Cleveland DW (1997) ALS-linked SOD1

mutant G85R mediates damage to astrocytes and promotes rapidly progressive disease with SOD1-containing inclusions. Neuron 18:327-338.

Buratti E, Baralle FE (2008) Multiple roles of TDP-43 in gene expression, splicing regulation, and human disease. Front Biosci 13:867-878.

Cairns NJ, Neumann M, Bigio EH, Holm IE, Troost D, Hatanpaa KJ, Foong C, White CL, 3rd, Schneider JA, Kretzschmar HA, Carter D, Taylor-Reinwald L, Paulsmeyer K, Strider J, Gitcho M, Goate AM, Morris JC, Mishra M, Kwong LK, Stieber A, Xu Y, Forman MS, Trojanowski JQ, Lee VM, Mackenzie IR (2007) TDP-43 in Familial and Sporadic Frontotemporal Lobar Degeneration with Ubiquitin Inclusions. Am J Pathol 171:227-240.

Chai A, Withers J, Koh YH, Parry K, Bao H, Zhang B, Budnik V, Pennetta G (2008) hVAPB, the causative gene of a heterogeneous group of motor neuron diseases in humans, is functionally interchangeable with its Drosophila homologue DVAP-33A at the Neuromuscular Junction. Hum Mol Genet 17:266-280.

De Vos KJ, Chapman AL, Tennant ME, Manser C, Tudor EL, Lau KF, Brownlees J, Ackerley S, Shaw PJ, McLoughlin DM, Shaw CE, Leigh PN, Miller CC, Grierson AJ (2007) Familial amyotrophic lateral sclerosis-linked SOD1 mutants perturb fast axonal transport to reduce axonal mitochondria content. Hum Mol Genet 16:2720-2728.

Feeney SJ, McKelvie PA, Austin L, Jean-Francois MJ, Kapsa R, Tombs SM, Byrne E (2001) Presymptomatic motor neuron loss and reactive astrocytosis in the SOD1 mouse model of amyotrophic lateral sclerosis. Muscle Nerve 24:1510-1519.

Fischer LR, Culver DG, Davis AA, Tennant P, Wang M, Coleman M, Asress S, Adalbert R, Alexander GM, Glass JD (2005) The WldS gene modestly prolongs survival in the SOD1G93A fALS mouse. Neurobiol Dis 19:293-300.

Fowler SC, Zarcone TJ, Vorontsova E, Chen R (2002) Motor and associative deficits in D2 dopamine receptor knockout mice. Int J Dev Neurosci 20:309-321.

Giordana MT, Piccinini M, Grifoni S, De Marco G, Vercellino M, Magistrello M, Pellerino A, Buccinna B, Lupino E, Rinaudo MT (2009) TDP-43 redistribution is an early event in sporadic amyotrophic lateral sclerosis. Brain Pathol.

Gitcho MA, Baloh RH, Chakraverty S, Mayo K, Norton JB, Levitch D, Hatanpaa KJ, White CL, 3rd, Bigio EH, Caselli R, Baker M, Al-Lozi MT, Morris JC, Pestronk A, Rademakers R, Goate AM, Cairns NJ (2008) TDP-43 A315T mutation in familial motor neuron disease. Ann Neurol 63:535-538.

Gitcho MA, Strider J, Carter D, Taylor-Reinwald L, Forman MS, Goate AM, Cairns NJ (2009) VCP mutations causing frontotemporal lobar degeneration disrupt localization of TDP-43 and induce cell death. J Biol Chem 284:12384-12398.

Gkogkas C, Middleton S, Kremer AM, Wardrope C, Hannah M, Gillingwater TH, Skehel P (2008) VAPB interacts with and modulates the activity of ATF6. Hum Mol Genet 17:1517-1526.

Igaz LM, Kwong LK, Xu Y, Truax AC, Uryu K, Neumann M, Clark CM, Elman LB, Miller BL, Grossman M, McCluskey LF, Trojanowski JQ, Lee VM (2008) Enrichment of C-Terminal Fragments in TAR DNA-Binding Protein-43 Cytoplasmic Inclusions in Brain but not in Spinal Cord of Frontotemporal Lobar Degeneration and Amyotrophic Lateral Sclerosis. Am J Pathol 173:182-194.

Ilieva HS, Yamanaka K, Malkmus S, Kakinohana O, Yaksh T, Marsala M, Cleveland DW (2008) Mutant dynein (Loa) triggers proprioceptive axon loss that extends survival only in the SOD1 ALS model with highest motor neuron death. Proc Natl Acad Sci USA 105:12599-12604.

Kabashi E, Valdmanis PN, Dion P, Spiegelman D, McConkey BJ, Velde CV, Bouchard JP, Lacomblez L, Pochigaeva K, Salachas F, Pradat PF, Camu W, Meininger V, Dupre N, Rouleau GA (2008) TARDBP mutations in individuals with sporadic and familial amyotrophic lateral sclerosis. Nat Genet 40:572-574.

Kanekura K, Nishimoto I, Aiso S, Matsuoka M (2006) Characterization of amyotrophic lateral sclerosis-linked P56S mutation of vesicle-associated membrane protein-associated protein B (VAPB/ALS8). J Biol Chem 28:30223-30232.

Kwiatkowski TJ, Jr., Bosco DA, LeClerc AL, Tamrazian E, Vanderburg CR, Russ C, Davis A, Gilchrist J, Kasarskis EJ, Munsat T, Valdmanis P, Rouleau GA, Hosler BA, Cortelli P, de Jong PJ, Yoshinaga Y, Haines JL, Pericak-Vance MA, Yan J, Ticozzi N, Siddique T, McKenna-Yasek D, Sapp PC, Horvitz HR, Landers JE, Brown RH, Jr. (2009) Mutations in the FUS/TLS Gene on Chromosome 16 Cause Familial Amyotrophic Lateral Sclerosis. Science 323:1205-1208.

Lalonde R, Strazielle C (2009) Exploratory activity and motor coordination in old versus middle-aged C57BL/6J mice. Arch Gerontol Geriatr 49:39-42.

Lee JH, Lau KF, Perkinton MS, Standen CL, Rogelj B, Falinska A, McLoughlin DM, Miller CC (2004) The neuronal adaptor protein X11beta reduces Abeta levels and amyloid plaque formation in the brains of transgenic mice. J Biol Chem 279:49099-49104.

Lee JH, Lau KF, Perkinton MS, Standen CL, Shemilt SJ, Mercken L, Cooper JD, McLoughlin DM, Miller CC (2003) The neuronal adaptor protein X11alpha reduces

Abeta levels in the brains of Alzheimer's APPswe Tg2576 transgenic mice. J Biol Chem 278:47025-47029.

Li Q, Lau A, Morris TJ, Guo L, Fordyce CB, Stanley EF (2004) A syntaxin 1, Galpha(o), and N-type calcium channel complex at a presynaptic nerve terminal: analysis by quantitative immunocolocalization. J Neurosci 24:4070-4081.

Loewen CJ, Levine TP (2005) A highly conserved binding site in VAP for the FFAT motif of lipid binding proteins. J Biol Chem 280:14097-14104.

Mackenzie IR, Bigio EH, Ince PG, Geser F, Neumann M, Cairns NJ, Kwong LK, Forman MS, Ravits J, Stewart H, Eisen A, McClusky L, Kretzschmar HA, Monoranu CM, Highley JR, Kirby J, Siddique T, Shaw PJ, Lee VM, Trojanowski JQ (2007) Pathological TDP-43 distinguishes sporadic amyotrophic lateral sclerosis from amyotrophic lateral sclerosis with SOD1 mutations. Ann Neurol 61:427-434.

McHanwell S, Biscoe TJ (1981) The sizes of motoneurons supplying hindlimb muscles in the mouse. Proc R Soc Lond B Biol Sci 213:201-216.

Mizuno Y, Amari M, Takatama M, Aizawa H, Mihara B, Okamoto K (2006) Immunoreactivities of p62, an ubiquitin-binding protein, in the spinal anterior horn cells of patients with amyotrophic lateral sclerosis. J Neurol Sci 249:13-18.

Nakajima R, Takao K, Huang SM, Takano J, Iwata N, Miyakawa T, Saido TC (2008) Comprehensive behavioral phenotyping of calpastatin-knockout mice. Mol Brain 1:7.

Neumann M, Sampathu DM, Kwong LK, Truax AC, Micsenyi MC, Chou TT, Bruce J, Schuck T, Grossman M, Clark CM, McCluskey LF, Miller BL, Masliah E, Mackenzie IR, Feldman H, Feiden W, Kretzschmar HA, Trojanowski JQ, Lee VM (2006) Ubiquitinated TDP-43 in frontotemporal lobar degeneration and amyotrophic lateral sclerosis. Science 314:130-113.

Nishimura AL, Mitne-Neto M, Silva HC, Richieri-Costa A, Middleton S, Cascio D, Kok F, Oliveira JR, Gillingwater T, Webb J, Skehel P, Zatz M (2004) A mutation in the vesicle-trafficking protein VAPB causes late-onset spinal muscular atrophy and amyotrophic lateral sclerosis. Am J Hum Genet 75:822-831.

Ou SH, Wu F, Harrich D, Garcia-Martinez LF, Gaynor RB (1995) Cloning and characterization of a novel cellular protein, TDP-43, that binds to human immunodeficiency virus type 1 TAR DNA sequence motifs. J Virol 69:3584-3596.

Pasinelli P, Brown RH (2006) Molecular biology of amyotrophic lateral sclerosis: insights from genetics. Nat Rev Neurosci 7:710-723.

Pennetta G, Hiesinger P, Fabian-Fine R, Meinertzhagen I, Bellen H (2002) Drosophila VAP-33A directs bouton formation at neuromuscular junctions in a dosage-dependent manner. Neuron 35:291-306.

Peretti D, Dahan N, Shimoni E, Hirschberg K, Lev S (2008) Coordinated lipid transfer between the endoplasmic reticulum and the Golgi complex requires the VAP Proteins and is essential for Golgi-mediated transport. Mol Biol Cell 19:3871-3884.

Prosser DC, Tran D, Gougeon PY, Verly C, Ngsee JK (2008) FFAT rescues VAPA-mediated inhibition of ER-to-Golgi transport and VAPB-mediated ER aggregation. J Cell Sci 121:3052-3061.

Puttaparthi K, Gitomer WL, Krishnan U, Son M, Rajendran B, Elliott JL (2002) Disease progression in a transgenic model of familial amyotrophic lateral sclerosis is dependent on both neuronal and non-neuronal zinc binding proteins. J Neurosci 22:8790-8796.

Ratnaparkhi A, Lawless GM, Schweizer FE, Golshani P, Jackson GR (2008) A Drosophila model of ALS: human ALS-associated mutation in VAP33A suggests a dominant negative mechanism. PLoS ONE 3:e2334.

Robertson J, Sanelli T, Xiao S, Yang W, Horne P, Hammond R, Pioro EP, Strong MJ (2007) Lack of TDP-43 abnormalities in mutant SOD1 transgenic mice shows disparity with ALS. Neurosci Lett 420:128-132.

Rogers DC, Fisher EM, Brown SD, Peters J, Hunter AJ, Martin JE (1997) Behavioral and functional analysis of mouse phenotype: SHIRPA, a proposed protocol for comprehensive phenotype assessment. Mamm Genome 8:711-713.

Seelaar H, Schelhaas HJ, Azmani A, Kusters B, Rosso S, Majoor-Krakauer D, de Rijik MC, Rizzu P, ten Brummelhuis M, van Doorn PA, Kamphorst W, Willemsen R, van Swieten JC (2007) TDP-43 pathology in familial frontotemporal dementia and motor neuron disease without Progranulin mutations. Brain 130:1375-1385.

Shan X, Vocadlo D, Krieger C (2009) Mislocalization of TDP-43 in the G93A mutant SOD1 transgenic mouse model of ALS. Neurosci Lett 458:70-74.

Skehel PA, Fabian-Fine R, Kandel ER (2000) Mouse VAP33 is associated with the endoplasmic reticulum and microtubules. Proc Natl Acad Sci USA 97:1101-1106.

Skehel PA, Martin KC, Kandel ER, Bartsch D (1995) A VAMP-binding protein from Aplysia required for neurotransmitter release. Science 269:1580-1583.

Sreedharan J, Blair IP, Tripathi VB, Hu X, Vance C, Rogelj B, Ackerley S, Durnall JC, Williams KL, Buratti E, Baralle F, de Belleroche J, Mitchell JD, Leigh PN, Al-Chalabi A, Miller CC, Nicholson G, Shaw CE (2008) TDP-43 Mutations in Familial and Sporadic Amyotrophic Lateral Sclerosis. Science 319:1688-1672.

Sumi H, Kato S, Mochimaru Y, Fujimura H, Etoh M, Sakoda S (2009) Nuclear TAR DNA binding protein 43 expression in spinal cord neurons correlates with the clinical course in amyotrophic lateral sclerosis. J Neuropathol Exp Neurol 68:37-47.

Suzuki H, Kanekura K, Levine TP, Kohno K, Olkkonen VM, Aiso S, Matsuoka M (2009) ALS-linked P56S-VAPB, an aggregated loss-of-function mutant of VAPB, predisposes motor neurons to ER stress-related death by inducing aggregation of co-expressed wild-type VAPB. J Neurochem 108:973-985.

Tan CF, Eguchi H, Tagawa A, Onodera O, Iwasaki T, Tsujino A, Nishizawa M, Kakita A, Takahashi H (2007) TDP-43 immunoreactivity in neuronal inclusions in familial amyotrophic lateral sclerosis with or without SOD1 gene mutation. Acta Neuropathol 113:535-542.

Teuling E, Ahmed S, Haasdijk E, Demmers J, Steinmetz MO, Akhmanova A, Jaarsma D, Hoogenraad CC (2007) Motor neuron disease-associated mutant vesicle-associated membrane protein-associated protein (VAP) B recruits wild-type VAPs into endoplasmic reticulum-derived tubular aggregates. J Neurosci 27:9801-9815.

Tsuda H, Han SM, Yang Y, Tong C, Lin YQ, Mohan K, Haueter C, Zoghbi A, Harati Y, Kwan J, Miller MA, Bellen HJ (2008) The amyotrophic lateral sclerosis 8 protein VAPB is cleaved, secreted, and acts as a ligand for Eph receptors. Cell 133:963-977.

Tudor EL, Perkinton MS, Schmidt A, Ackerley S, Brownlees J, Jacobsen NJ, Byers HL, Ward M, Hall A, Leigh PN, Shaw CE, McLoughlin DM, Miller CC (2005) ALS2/ALSIN regulates RAC-PAK signalling and neurite outgrowth. J Biol Chem 280:34735-34740.

Turner BJ, Baumer D, Parkinson NJ, Scaber J, Ansorge O, Talbot K (2008) TDP-43 expression in mouse models of amyotrophic lateral sclerosis and spinal muscular atrophy. BMC Neurosci 9:104.

Valdmanis PN, Rouleau GA (2008) Genetics of familial amyotrophic lateral sclerosis. Neurology 70:144-152.

Van Deerlin VM, Leverenz JB, Bekris LM, Bird TD, Yuan W, Elman LB, Clay D, Wood EM, Chen-Plotkin AS, Martinez-Lage M, Steinbart E, McCluskey L, Grossman M, Neumann M, Wu IL, Yang WS, Kalb R, Galasko DR, Montine TJ, Trojanowski JQ, Lee VM, Schellenberg GD, Yu CE (2008) TARDBP mutations in amyotrophic lateral sclerosis with TDP-43 neuropathology: a genetic and histopathological analysis. Lancet Neurol 7:409-416.

Vance C, Rogelj B, Hortobagyi T, De Vos KJ, Nishimura AL, Sreedharan J, Hu X, Smith B, Ruddy D, Wright P, Ganesalingam J, Williams KL, Tripathi V, Al-Saraj S, Al-Chalabi A, Leigh PN, Blair IP, Nicholson G, de Belleroche J, Gallo J-M, Miller CC, Shaw CE (2009) Mutations in FUS, an RNA Processing Protein, Cause Familial Amyotrophic Lateral Sclerosis Type 6. Science 323:1208-1211.

Wang IF, Reddy NM, Shen CK (2002) Higher order arrangement of the eukaryotic nuclear bodies. Proc Natl Acad Sci USA 99:13583-13588.

Winton MJ, Igaz LM, Wong MM, Kwong LK, Trojanowski JQ, Lee VM (2008a) Disturbance of nuclear and cytoplasmic Tar DNA binding protein (TDP-43) induces disease-like redistribution, sequestration and aggregate formation. J Biol Chem 283:13302-13309.

Winton MJ, Van Deerlin VM, Kwong LK, Yuan W, Wood EM, Yu CE, Schellenberg GD, Rademakers R, Caselli R, Karydas A, Trojanowski JQ, Miller BL, Lee VM (2008b)

A90V TDP-43 variant results in the aberrant localization of TDP-43 in vitro. FEBS Lett 582:2252-2256.

Yokoseki A, Shiga A, Tan CF, Tagawa A, Kaneko H, Koyama A, Eguchi H, Tsujino A, Ikeuchi T, Kakita A, Okamoto K, Nishizawa M, Takahashi H, Onodera O (2008) TDP-43 mutation in familial amyotrophic lateral sclerosis. Ann Neurol 63:538-542.

Zhou C, Zhao CP, Zhang C, Wu GY, Xiong F (2007) A method comparison in monitoring disease progression of G93A mouse model of ALS. Amyotroph Lateral Scler 8:366-372.

Figure Legends

Figure 1

Transgene expression in VAPBwt and VAPBP56S transgenic mice. Total protein samples of spinal cord (A) and brain (B) from non-transgenic (NTg), the two different VAPBwt transgenic (VAPBwt 1 and 2), and the two different VAPBP56S (VAPBP56S 1 and 2) transgenic lines used in the study were probed on immunoblots for total VAPB and transgene-derived VAPB (using antibody 9B11 to the myc tag). The blots were also probed for tubulin as a loading control. 10 µg of protein is loaded in each track.

Figure 2

Immunohistochemical detection of VAPBwt and VAPBP56S in lumbar spinal cords and brains of 18 month old transgenic mice. (A-C) show spinal cords of non-transgenic (NTg) (A), VAPBwt (B) and VAPBP56S (C) transgenic mice labelled with antibody 9E10 to the myc tag (myc) or rabbit anti-VAPB antibody (VB) as indicated. Lower magnification images are shown on the left; motor neurons in ventral horns are shown at higher magnification on the right. (D and E) show cerebral cortex in brains of non-transgenic (NTg), VAPBwt and VAPBP56S transgenic mice labelled with antibody 9E10 to the myc tag as indicated. Lower magnification images are shown in (D); higher magnification images in (E). Note the punctate aggregates seen with the myc antibody in VAPBP56S mice in the higher magnification images of both spinal cord and brain (arrowheads in C and E). Scale bars: (A-C), 350 µm (low magnification –left images) and 15 µm (high magnification -right images); (D), 30 µm; (E) 10 µm.

Figure 3

VAPBP56S but not VAPBwt transgenic mice develop cytoplasmic ubiquitin accumulations. (A) shows ventral horn regions in lumbar spinal cords of 18 month old non-transgenic (NTg), VAPBwt and VAPBP56S mice, and 16 week old SOD1G93A transgenic mice labelled for ubiquitin with antibody Ubi-1 as indicated. (B) and (C) show motor neurons in ventral horns of 18 month old non-transgenic (NTg), VAPBwt and VAPBP56S transgenic mice labelled for ubiquitin (B) and p62 (C) as indicated. Note the selective prominent cytoplasmic ubiquitin/p62 labelling in spinal cord motor neurons in VAPBP56S transgenic mice (arrowheads in B and C). Scale bars: (A), 50 µm; (B) and (C), 15 µm.

Figure 4

VAPBP56S but not VAPBwt transgenic mice develop cytoplasmic TDP-43 pathology. (A) shows ventral horn regions in lumbar spinal cords of 18 month old non-transgenic (NTg), VAPBwt and VAPBP56S mice, and 16 week old SOD1G93A transgenic mice labelled for TDP-43 as indicated. (B) shows high power images of motor neurons in ventral horns of 18 month old non-transgenic (NTg), VAPBwt and VAPBP56S transgenic mice labelled for TDP-43. In VAPBP56S mice granular structures and occasional small paranuclear inclusions were detected. In addition, diffuse cytoplasmic TDP-43 labelling was also seen along with some reduction in nuclear labelling (see lower centre image). Skeins and large round inclusions as seen in human ALS cases were not observed. (C) shows TDP-43 labelling in ventral spinal cord of a human fronto-temporal lobar degeneration with ALS case for comparison. Note the numerous large and intensely stained skein-like, filamentous, round and irregular cytoplasmic TDP-43 inclusions (arrowheads). Scale bars: (A), 50 µm; (B,C) 10 µm; (D), 40 µm (low magnification –left image), 15 µm (high magnification –right image).

Figure 5

Associations of cytoplasmic TDP-43 and VAPB with ubiquitin in VAPBP56S transgenic motor neurons. Ventral horn motor neurons from lumbar spinal cords of 18 month old VAPBwt (A) and VAPBP56S (B) mice were triple stained for VAPB (rat antibody; green), ubiquitin (mouse antibody; yellow), and TDP-43 (rabbit antibody; red) and imaged by confocal microsocopy. Image correlation analyses of ubiquitin and TDP43 (C), and ubiquitin and VAPB (D) are illustrated for a region of interest taken from B (arrowed in B). The product of the difference from the mean (PDM=(A-a)(B-b), where A and B are the pixel values and a and b their respective means) was calculated for each pixel pair derived from the 2 image channels under investigation, TDP43 and ubiquitin (C), or VAPB and ubiquitin (D). Positive pixel pairs that yielded a positive PDM, indicating co-localisation, along with individual channels (TDP-43, ubiquitin and VAPB) and overlays (Merge) are shown in (C) and (D). Scatter plots (Scatter) showing the relationships between the pixels intensities of TDP-43 and ubiquitin, and VAPB and ubiquitin are shown in the right-hand plot panels of (C) and (D) respectively. ICA plots of normalized TDP-43 (C, left) and ubiquitin (C, right), and VAPB (D, left) and ubiquitin (D, right) versus their respective PDM ((A-a)(B-b)) values are shown. Note the positively skewed intensity versus PDM plots in panel C, and D, indicative of association of TDP-43 and ubiquitin, and VAPB and ubiquitin, respectively. The TDP-43/ubiquitin ICA plots are more positively skewed than the VAPB/ubiquitin plots in line with the higher association between TDP-43 and ubiquitin. Scale bar=10 μm.

Figure 6

Absence of TDP-43 processing in VAPBP56S transgenic mice. Immunoblots of TDP-43 in spinal cords and brains of different 24 month old non-transgenic (NTg), VAPBwt and

VAPBP56S transgenic mice as indicated.

Figure 1

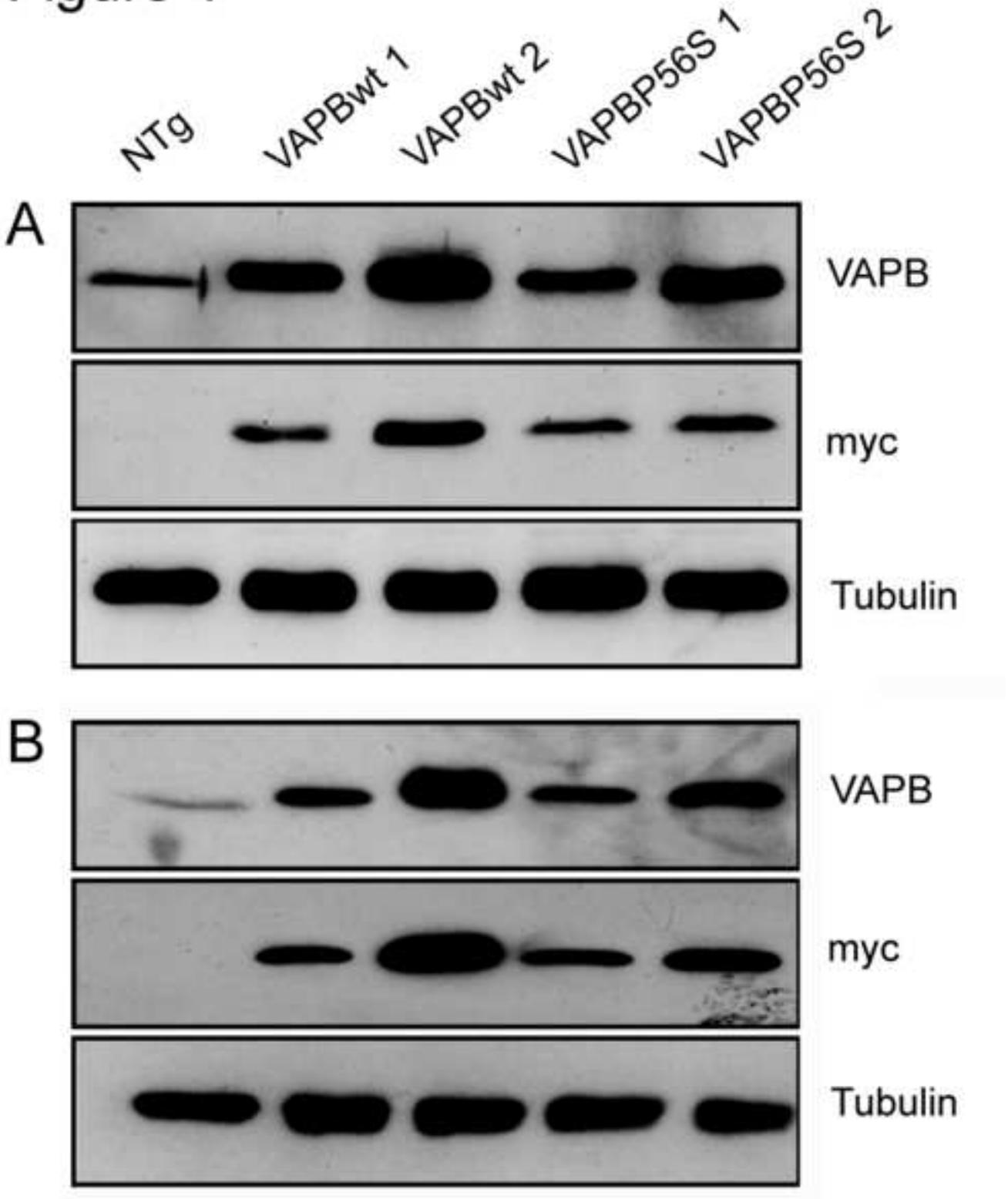

Figure 2

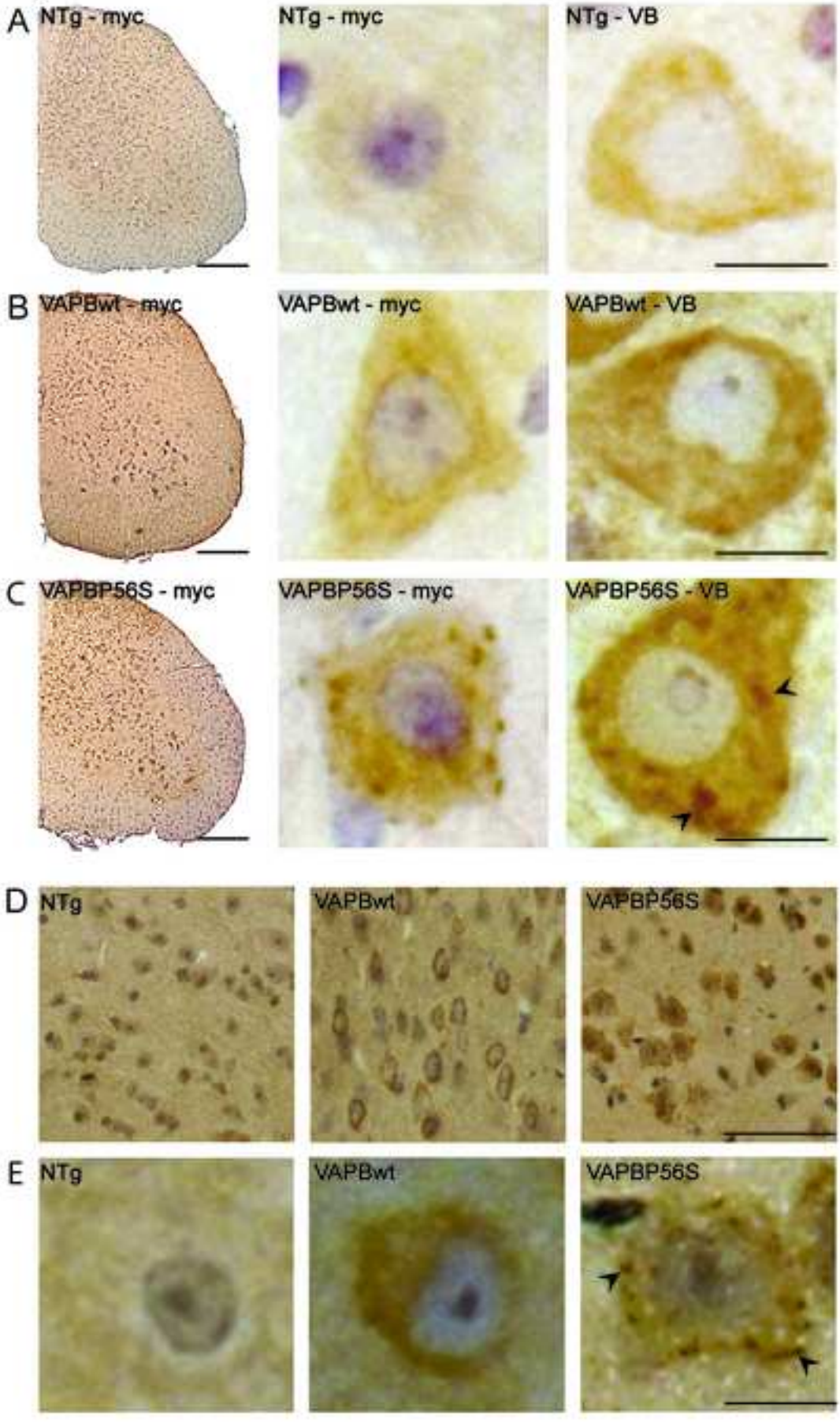

Figure 3

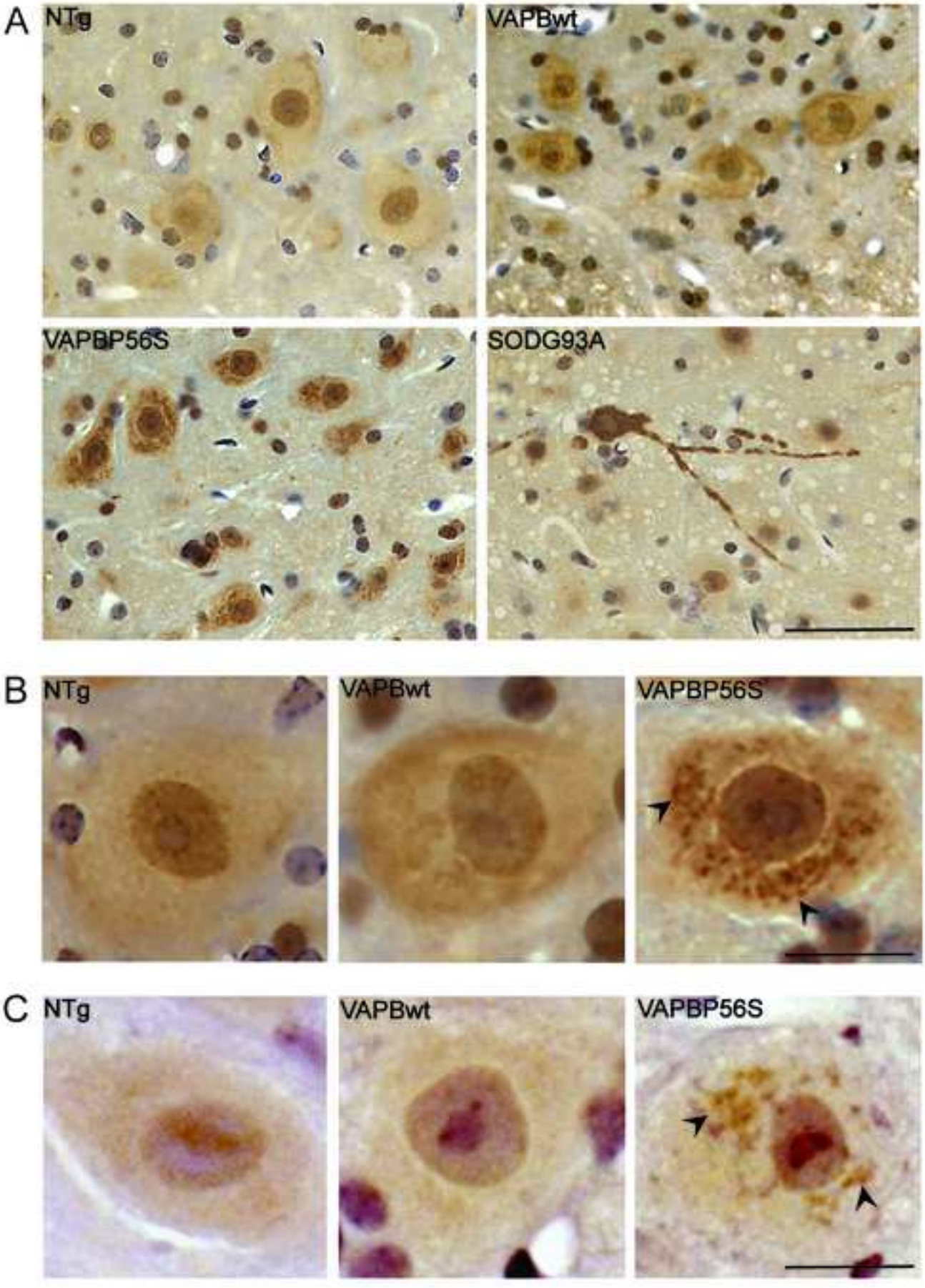

Figure 4

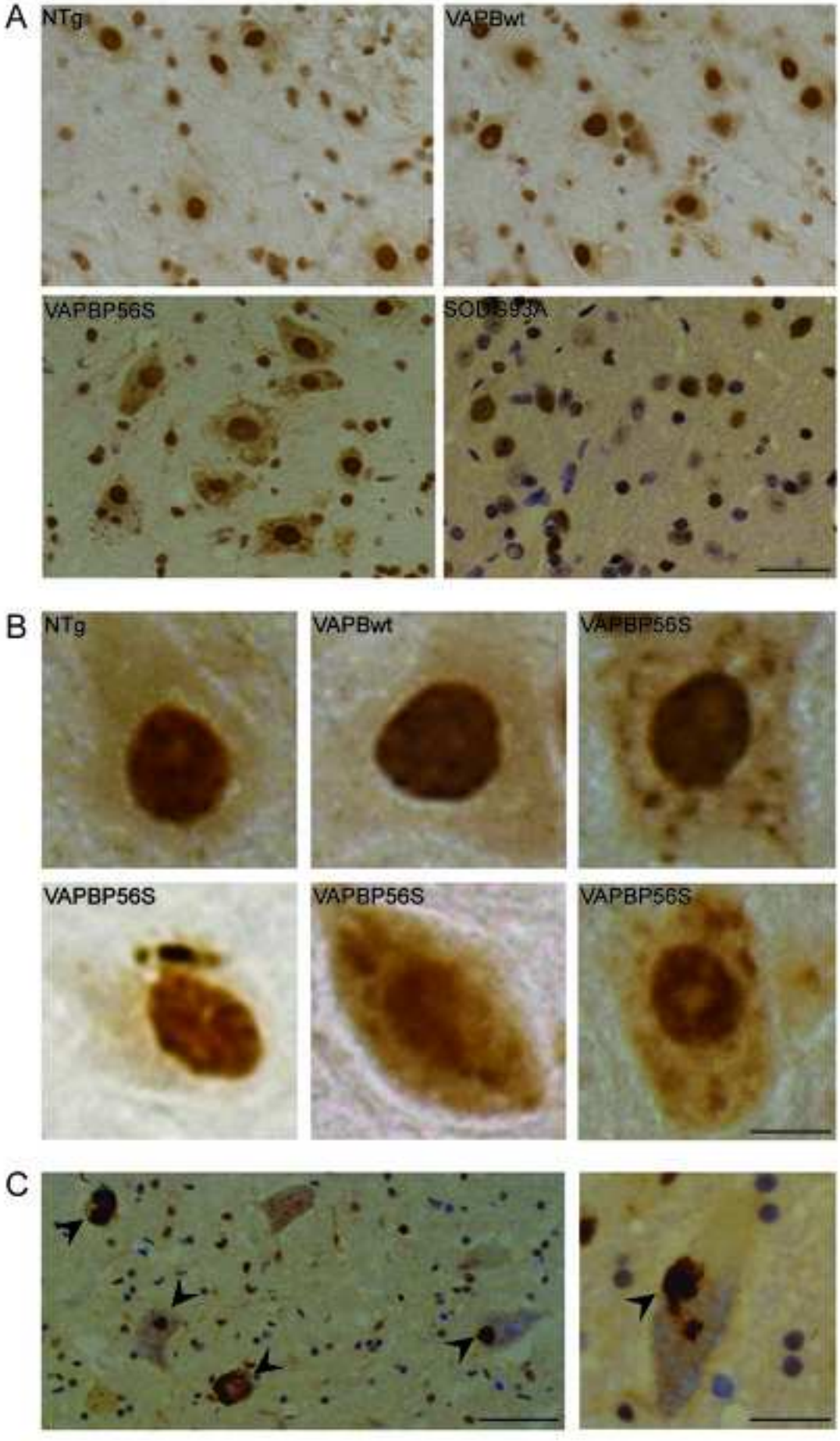

Figure 5

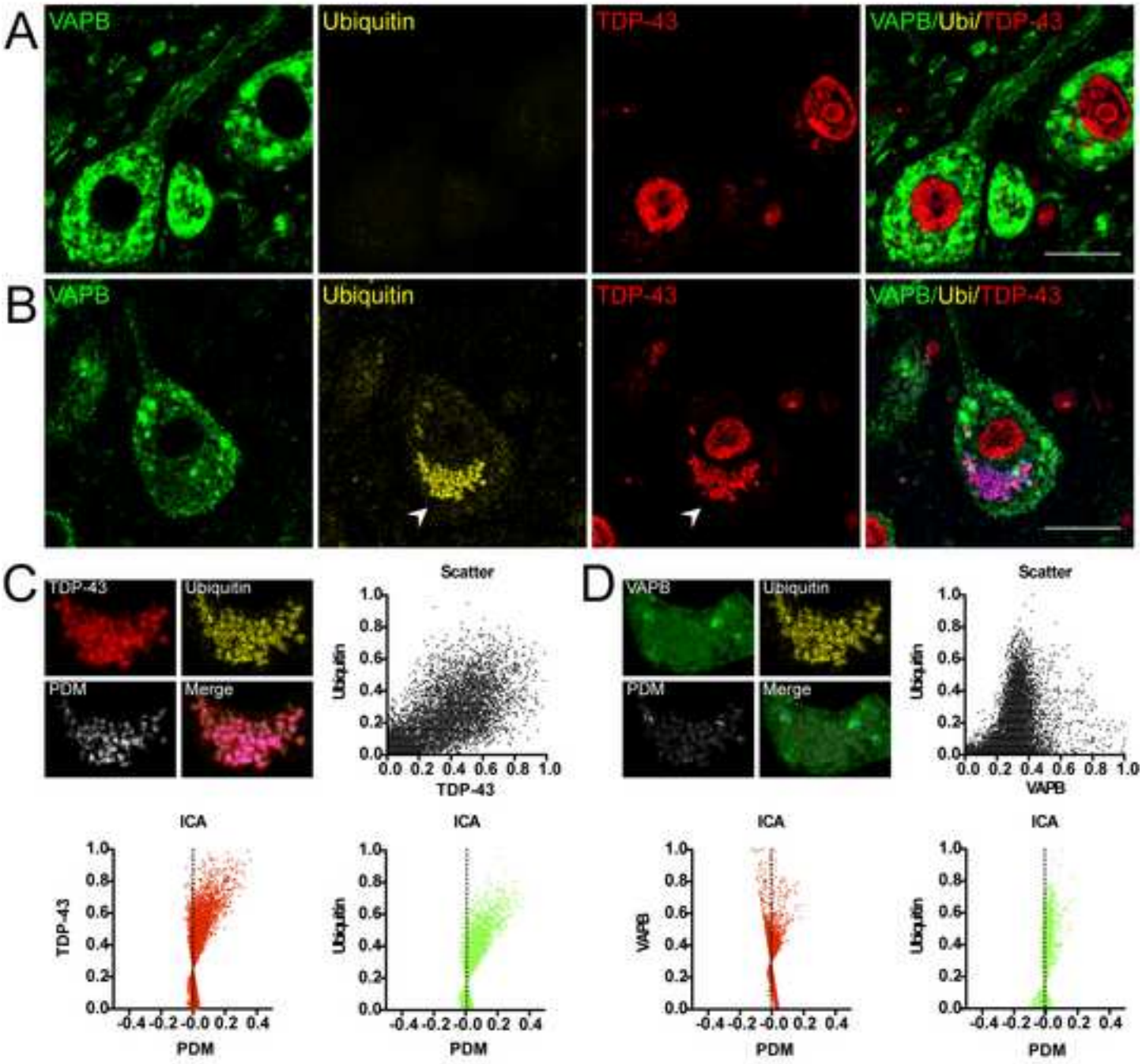

Figure
Click here to download high resolution image

Figure 6